Manoeuvrability Assessment of a Hybrid Compound Helicopter Configuration

Kevin Ferguson

Ph.D Student,

University of Glasgow,

James Watt South Building, Glasgow

Douglas Thomson

Senior Lecturer,

University of Glasgow,

James Watt South Building, Glasgow

Abstract

The compound helicopter design could potentially satisfy the new emerging requirements placed on the next generation of rotorcraft. The main benefit of the compound helicopter is its ability to reach speeds that significantly surpass the conventional helicopter. However, it is possible that the compound helicopter design can provide additional benefits in terms of manoeuvrability. The paper features a conventional helicopter and a hybrid compound helicopter. The conventional helicopter features a standard helicopter design with a main rotor providing the propulsive and lifting forces, whereas a tail rotor, mounted at the rear of the aircraft provides the yaw control. The compound helicopter configuration, known as the hybrid compound helicopter, features both wing and thrust compounding. The wing offloads the main rotor at high speeds whereas two propellers provide additional axial thrust as well as yaw control. This study investigates the manoeuvrability of these two helicopter configurations using inverse simulation. The results predict that a hybrid compound

Presented at the 40th European Rotorcraft Forum, Southampton, U.K., September 2-5th, 2014.

helicopter configuration is capable of attaining greater load factors than its conventional counterpart, when flying a Pullup-Pushover manoeuvre. In terms of the Accel-Decel man oeuvre, the two helicopter configurations are capable of completing the manoeuvre in comparable time-scales. However, the addition of thrust compounding to the compound helicopter design reduces the pitch attitude required throughout the acceleration stage of the manoeuvre.

Nomenclature

g	acceleration due to gravity (m/s^2)
k	time point counter
n_{max}	maximum normal load factor
n_p	normal load factor
$\bar{r}$	radial station along the rotor blade
S	Accel-Decel distance (m)
t	time (s)
$\mathbf{u}$	control vector (rad)
V	aircraft flight speed (m/s)
$\dot{V}$	aircraft acceleration (m/s^2)
x, y, z	manoeuvre flight path co-ordinates (m)
$\mathbf{x}$	state vector (various units)
$\dot{x}, \dot{y}, \dot{z}$	earth axes velocities (m/s)
$\ddot{x}, \ddot{y}, \ddot{z}$	earth axes accelerations (m/s^2)
$\mathbf{y}_{des}$	trajectory definition matrix (various units)
α_e	trimmed fuselage angle of attack (rad)
α_{max}	maximum local rotor blade angle of attack at $\bar{r} = 0.8$ (rad)
α'	fuselage angle of attack excursion (rad)

χ track angle (rad)

γ glideslope angle (rad)

$\dot{\gamma}$ time derivative of the glideslope angle (rad/s)

ψ heading angle (rad)

θ Euler pitch angle (rad)

θ_0 main rotor collective pitch angle (rad)

θ_{1s} main rotor longitudinal pitch angle (rad)

θ_{1c} main rotor lateral pitch angle (rad)

θ_{diff} propellers differential control pitch angle (rad)

$\bar{\theta}_{prop}$ mean propeller pitch angle (rad)

Introduction

The compound helicopter has experienced a resurgence of interest due to its ability to obtain speeds that significantly surpass the conventional helicopter. This increase in speed, provided that efficient hover capability is maintained, would make the compound helicopter suitable for various roles and missions such as troop insertion, search and rescue, ship replenishment as well as short haul flights in the civil market. The compounding of a helicopter is not a new idea but the development of a compound helicopter has proven elusive for the rotorcraft community due to a combination of technical problems and economical issues [1]. The rotorcraft community is again exploring the compound helicopter design, with various manufacturers testing their prototypes.

The success of the conventional helicopter is partly due to its unique ability to perform precise manoeuvres in Nap of the Earth (NAP) flight. One method of assessing the helicopter's ability to perform manoeuvres is inverse simulation. Inverse simulation reverses the conventional simulation approach by calculating the control activity required to force a vehicle along a particular trajectory [2]. The first inverse simulation algorithm, known as the differentiation method, was developed by Thomson and Bradley [3], to assess helicopter agility of a six degree of freedom (DOF) rotorcraft model. The success of the inverse simulation results, as well as the increasing interest in handling qualities and pilot workload research,

prompted future development of the algorithm. Subsequently, inverse simulation has been used for various applications, including investigating pilot control strategies, conceptual design analyses and handling qualities [4–7]. Despite the success of the differentiation method, there were some problems which consequently led to a new approach to inverse simulation. The major limitation of the differentiation method was that the mathematical model and the algorithm were strongly coupled, therefore even slight changes to the mathematical model required alterations to the algorithm itself. Realizing this shortcoming, Hess, Goa and Wang developed a generalized technique of inverse simulation [8], often referred to as the integration method, which fully separates the mathematical model from the algorithm. Due to the robust and flexible nature of this technique, the integration method has become the most common approach [9]. Before proceeding, another two methods of solving the inverse problem should be noted. Firstly, the two time-scale method, as described by Avanzini, de Matteis and de Socio [10, 11], assumes that the rotational dynamics of an aircraft are much quicker than the translational dynamics, therefore permitting the assumption that the main rotor collective controls the translational dynamics whereas the cyclic and pedals influence the rotational dynamics. This method, similar to the other methods, use iterative schemes, such as the Newton-Raphson method, in order to solve the inverse problem. However, the Newton-Raphson method can be replaced with an optimization algorithm in order to calculate the control angles, with Celi and de Matteis et al. [12, 13] successfully implementing optimization algorithms in their respective approaches. The optimization approach to inverse simulation is particularly useful to problems featuring control redundancy, however an appropriate cost function must be formed.

In terms of manoeuvrability, it is an important design feature if the helicopter is to operate in tight Nap of the Earth (NoE) scenarios [14]. The ability for the helicopter to manoeuvre quickly and effectively enables the vehicle to quickly re-position. Furthermore, enhancing the maneuverability and agility of a helicopter can also aid its survivability with its ability to quickly turn or climb to avoid an attack. Traditionally, the design process has focused on performance and cost to drive the design of the helicopter. However, for the reasons previously stated, a high level of maneuverability has become a key design goal for most designers as it increases mission effectiveness [15]. As there is a demand for conventional helicopters to be manoeuvrable, it is reasonable to expect that operators would expect the same for a compound helicopter. Therefore, this paper presents a manoeuvrability assessment of a compound helicopter

and compares the results to a conventional helicopter of similar shape and mass. Before proceeding it is important to highlight that there are various definitions of the term manoeuvrability. Therefore it is necessary to define what is meant by manoeuvrability in this current work. Generally, most authors agree that manoeuvrability is the ability of the aircraft to change its flight path [14, 16] with Whalley [17] providing an overview of the various definitions proposed by authors. Whalley also concludes by stating his definition of manoeuvrability, which is the following

"Manoeuvrability is the measure of the maximum achievable time-rate-of-change of velocity vector at any point in the flight envelope."

The aim of the current work is to determine the maximum manoeuvring capability of two aircraft configurations, namely a conventional helicopter configuration and a hybrid compound helicopter configuration. Then to subsequently investigate if the compounding of the conventional helicopter offers an advantage in this regard. Hence, in this context, the term "manoeuvrability" and phrase "maximum manoeuvring capability" are used synonymously throughout the remainder of this paper. The strategy for the current work is to use an established mathematical model of a conventional helicopter (in this case, the AgustaWestland Lynx, as seen in Figure 1(a)), and then convert this model to represent a hybrid compound helicopter configuration. The Lynx was chosen as the starting point as a well established dataset and model was available [18]. The compound configuration that is examined in the paper is broadly similar to the Eurocopter X^3 with the preliminary design of the configuration discussed in a previous compound helicopter study [19]. This configuration is named the hybrid compound helicopter (HCH) configuration, which features a wing and two propellers, as seen in Figure 1(b). This compound helicopter configuration is changed as little as possible, relative to the baseline model, to allow for a fair and direct comparison between the results of the two configurations. The result is a rather unusual looking vehicle, Figure 1(b); however, it should be stressed that this is not a design exercise but a study to investigate the influence of compounding. Therefore to ensure that the effects of compounding are isolated from other factors, the basic vehicle shape and size is maintained. The approach in this work is to use inverse simulation to quantify the manoeuvrability of the aircraft configurations. This requires various elements such as helicopter mathematical models, inverse simulation algorithm, modelling of helicopter manoeuvres and a manoeuvrability assessment method. The following section provides an overview of these required

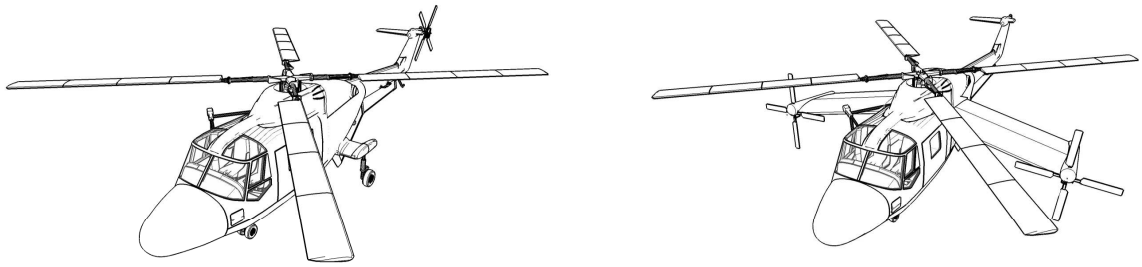

(a) Baseline Helicopter Sketch (b) Hybrid Compound Helicopter Sketch

Fig. 1 Sketches of the two Helicopter Configurations

elements.

Methodology

Helicopter Mathematical Modelling

The compound helicopter model is developed using the helicopter generic simulation (HGS) model [20]. The HGS model is a conventional disc-type rotorcraft model, as described by Padfield [18], and has found extensive use in studies of helicopter flight dynamics. The HGS model is generic in structure, with only the helicopter's parameters required to model the vehicle. The main rotor model, within the HGS package, ignores the pitching and lagging degrees of freedom, therefore assuming that the flap dynamics have the most influence in terms of the helicopter's flight dynamic characteristics. The flapping dynamics are assumed to be quasi steady, a common assumption in main rotor modelling, therefore permitting a multi-blade representation of the main rotor. The rotor model neglects the rotor periodicity by assuming that only the steady components of the periodic forces and moments generated by the main rotor influence the helicopter's body dynamics. The main rotor is assumed to be centrally hinged with stiffness in flap, with the main rotor chord assumed to be constant. Furthermore, the model also features dynamic inflow and a rotor-speed governor model. One important assumption, within the rotor model, is that the aerodynamics are linear, so that the lift is a linear function of the local blade angle of attack, whereas the drag is mod-

elled by a simple polynomial. Due to this assumption, nonlinear aerodynamics such as retreating blade stall and compressibility are not modelled. To model the nonlinear aerodynamics and rotor periodicity requires an "individual blade model,", examples of which are given by Kim et.al, Rutherford, Mansur and Houston [21–24]. Regarding the modelling of the other subsystems of the rotorcraft, the forces and moments of the tail plane, fuselage, and fin are calculated using a series of lookup tables derived from experimental data [18].

One question that naturally arises is the validity of these models and if the results from these rotorcraft models would replicate the real aircraft. In terms of the conventional helicopter, inverse simulation results have shown good correlation for a range of manoeuvres [25], giving confidence to the worth of the results produced by the HGS model. The limitations of this type of model are well understood [18] and include the inability to accurately capture off-axis effects and low fidelity at the edges of the flight envelope where, for example, aerodynamic are highly nonlinear. In relation to the compound helicopter models, a strict validation based on the comparison of flight test with simulation results is not possible, as the appropriate data is not yet openly available. However, it is believed that the mathematical models would correctly represent the basic physics of the hybrid compound helicopter.

Inverse Simulation Algorithm

The inverse simulation algorithm used in this current study is the so called integration method. As this method is well documented in the literature [2, 9, 26] only a brief description is provided within. The integration method uses numerical integration and conventional simulation to calculate the controls required to move a vehicle through a desired trajectory. The first step is to calculate the control angles that trim the aircraft for the given starting flight speed. Generally, a helicopter can be in trimmed flight when climbing, descending or flying with a lateral velocity (sideslip). However in this current work the trimmed state corresponds to steady level flight with the body accelerations and the attitude rates equal to zero. The next step, after the calculation of the trim control angles is to define the manoeuvre. The manoeuvre is discretised into a series of discrete time points, t_k, by specifying the time step and calculating the number of points. Subsequently, the manoeuvre can be determined with matrix, $\mathbf{y}_{des}(t_k)$ representing the flight

path of the manoeuvre. The manoeuvre can be defined by polynomials that satisfy the requirements of the particular manoeuvre [27], with the mathematical modelling of these manoeuvres detailed later. Starting from the trimmed condition, $\mathbf{u}_e$ is the initial guess to calculate the control vector, $\mathbf{u}$, to force the helicopter to the position of the next time point. A Newton-Raphson technique is used to calculate the control vector to force the vehicle to the next time point to match the desired flight path defined by $\mathbf{y}_{des}(t_k)$. After convergence, this numerical technique moves onto the next time point and repeats the process. The end result is the control activity required throughout the manoeuvre.

ADS-33 Maneuver Modeling

ADS-33 Pullup-Pushover Maneuver

Of course to successfully implement inverse simulation requires the trajectory the aircraft is to follow. In the early inverse simulation algorithms the output vector, which describes the trajectory, was defined as follows

$$\mathbf{y}_{des} = [x_e \quad y_e \quad z_e \quad \psi]^T \tag{1}$$

where x_e, y_e and z_e are the flight path co-ordinates and the additional constraint, ψ, is the heading angle. However with this form of output vector the calculated control activity contained high frequency oscillations [2]. By modifying the output vector to the following

$$\mathbf{y}_{des} = [\ddot{x}_e \quad \ddot{y}_e \quad \ddot{z}_e \quad \dot{\psi}]^T \tag{2}$$

was shown to attenuate these oscillations [22]. Therefore, in this current work the output vector consists of the aircraft accelerations and heading rate. The accelerations are determined by the differentiation of the velocities in the Earth axes set, which are given by

$$\dot{x} = V\cos\gamma\cos\chi \tag{3}$$

$$\dot{y} = V\cos\gamma\sin\chi \tag{4}$$

$$\dot{z} = -V\sin\gamma \tag{5}$$

leading to the following accelerations

$$\ddot{x} = \dot{V}\cos\gamma\cos\chi - V\dot{\gamma}\sin\gamma\cos\chi - V\dot{\chi}\cos\gamma\sin\chi \tag{6}$$

$$\ddot{y} = \dot{V}\cos\gamma\sin\chi - V\dot{\gamma}\sin\gamma\sin\chi + V\dot{\chi}\cos\gamma\cos\chi \tag{7}$$

$$\ddot{z} = -\dot{V}\sin\gamma - V\dot{\gamma}\cos\gamma \tag{8}$$

It is therefore clear that if the flight speed and trajectory angle profiles are known then the accelerations in the Earth axes set can be determined. In contrast, if expressions of x_e, y_e and z_e as a function of time are available then the accelerations can be determined easily without the use of Equation (6)- (8). However, the general case is that the accelerations can be obtained by specifying the flight speed and trajectory angles throughout the manoeuvre.

The manoeuvres studied with this paper are typical conventional helicopter manoeuvres, similar to the Pullup-Pushover and Accel-Decel manoeuvres described in the ADS-33 [28] requirements. The Pullup-Pushover manoeuvre involves the aircraft achieving positive and negative load factors. The objective of the Pullup-Pushover manoeuvre, as described in ADS-33 [28], is to examine the ability of the aircraft to avoid obstacles during high speed NoE operations. The aircraft begins the manoeuvre at a trimmed condition at a flight speed equal or less to 120 kt. In the pull up stage of the manoeuvre the aircraft is required to achieve a positive normal load factor and maintain this for a given period of time. Following this the aircraft is then to transition to a pushover and achieve a negative load factor then to recover to level flight as quickly as possible. The normal load factor is defined as

$$n_p = 1 - \frac{\ddot{z}}{g} \tag{9}$$

and the rearrangement of Equation (5) gives the standard definition of the glideslope angle

$$\gamma = -\sin^{-1}\frac{\dot{z}}{V} \tag{10}$$

The time derivative of the glideslope is therefore

$$\dot{\gamma} = \frac{-\ddot{z}V + \dot{V}\dot{z}}{V^2\cos\gamma} \tag{11}$$

Through the use of Equations (9) and (11), the time derivative of the glideslope angle can be expressed in terms of the normal load factor and flight speed as

$$\dot{\gamma} = \frac{\dot{V}\dot{z} - V(g - gn_p)}{V^2\cos\gamma} \tag{12}$$

The next step is to define the load factor distribution throughout the manoeuvre by applying the manoeuvre boundary conditions. The ADS-33 document specifies the majority of the load factors to be attained throughout the manoeuvre [28]. To meet the desired standards of this manoeuvre, the maximum positive load factor must be attained after 1s of commencing the manoeuvre and sustained for a further 2s. Thereafter, the helicopter transitions from the positive load factor to the lowest load factor within 2s, and maintains this load factor for a further 2s. Figure 2 shows a typical load factor distribution which relates to the desirable standards set in the specification with Table 1 providing the manoeuvre boundary conditions. The specification does not explicitly define an end time of the manoeuvre, a point raised by Celi [29], but does state that after the pushover stage of the manoeuvre the aircraft should "*recover to level flight as rapidly as possible*". The assumption in this current work is that the manoeuvre ends when the aircraft's original flight speed is recovered at $t = t_5$ with the normal load factor returning to unity and sustained at this value for a further 2s until $t = t_6$. By using the boundary conditions, as seen in Table 1, between each of the manoeuvre segments a fifth-order polynomial is formed to describe the load factor distribution

$$n_p = a_0t^5 + a_1t^4 + a_2t^3 + a_3t^2 + a_4t + a_5 \tag{13}$$

Once the coefficients, a_0, a_1, a_2, a_3, a_4 and a_5, are determined by applying the boundary conditions then the normal load factor distribution throughout the manoeuvre can be calculated. The next step is to

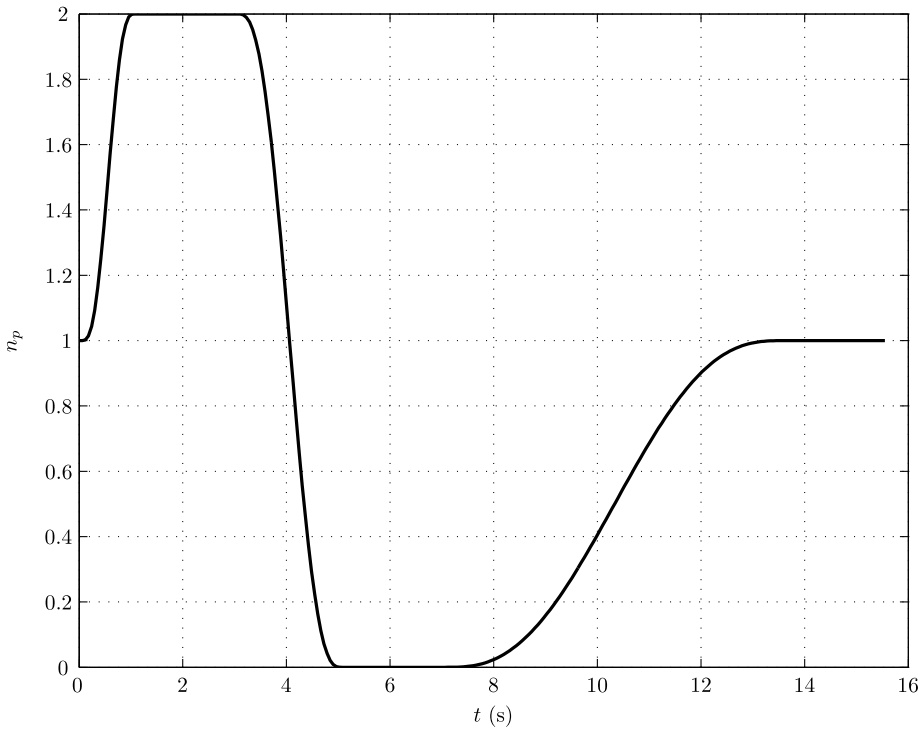

Fig. 2 Desirable Load Factor throughout the Pullup-Pushover maneuver.

determine the variation of flight speed throughout the manoeuvre. One solution to this is to impose a predetermined profile of flight speed throughout the manoeuvre, however there is very little information regarding the variation of airspeed throughout this manoeuvre. The approach taken in this present work, in

Table 1. Load Factor Boundary Conditions

Variable	$t = 0s$	$t = t_1$	$t = t_2$	$t = t_3$	$t = t_4$	$t = t_5$	$t = t_6$
n_p	1	n_{max}	n_{max}	0	0	1	1
$\dot{n}_p$	0	0	0	0	0	0	0
$\ddot{n}_p$	0	0	0	0	0	0	0
α	α_e	$\alpha_e + \alpha^{'}$	$\alpha_e + \alpha^{'}$	$\alpha_e - \alpha^{'}$	$\alpha_e - \alpha^{'}$	α_e	α_e

order to determine a flight speed profile, is to assume that there is a balance of potential and kinetic energy during the manoeuvre. For example, when the aircraft climbs there is a gain in potential energy which is balanced by a loss of kinetic energy. This assumption of the balance of energy leads to the following equation

$$\dot{V} = -g \sin \gamma \tag{14}$$

The result is that as the aircraft climbs airspeed reduces whereas as the vehicle descends then airspeed increases. There are now two differential equations, Equations (12) and (14), which can be integrated to determine the flight velocity and climb angle throughout the manoeuvre, using the initial trimmed conditions. As the track angle, χ is set to zero since it is a longitudinal manoeuvre, using the calculated values of V, $\dot{V}$, γ and $\dot{\gamma}$ the accelerations in the Earth axes set can be determined. Recall that the time derivative of the heading angle, $\dot{\psi}$, is constrained throughout the manoeuvre and set to zero.

As previously discussed, $\mathbf{y}_{des}$ is composed of the accelerations of $\ddot{x}_e$, $\ddot{y}_e$ and $\ddot{z}_e$ relative to the Earth axes set. Furthermore, since the conventional helicopter features four controls then the condition of zero heading or sideslip is included so that the output vector contains four elements. However, the 5 controls of the HCH configuration presents an issue in order to calculate a unique solution of the control vector at each time point. One solution is to include an additional constraint in the output vector to match the 5 controls of the compound helicopter configuration. In terms of the Pullup-Pushover manoeuvre, the extra constraint is selected to be the time derivative of the fuselage angle of attack, $\dot{\alpha}$. Conversely, an alternative approach could have been to schedule a control such as θ_{1s} throughout the manoeuvre. However, the justification of the inclusion of an additional constraint with scheduling $\dot{\alpha}$ across the manoeuvre is that it is likely a pilot would adopt a control strategy which exploits the lifting capability of the wing in the pull up stage of the manoeuvre. It is found by experimentation by including $\dot{\alpha}$ as an additional constraint and appropriately scheduling this value over the duration of the manoeuvre results in the wing supplementing the main rotor to achieve positive and negative load factors. Table 1 shows the distribution of the fuselage angle of attack, starting at its trim value of α_e before increasing to a value of $\alpha_0 + \alpha^{'}$. This increase of the fuselage angle of attack in the pull up stage of the manoeuvre increases the wing's lifting force helping

the vehicle create a positive load factor. Similarly in the pushover stage of the manoeuvre the wing helps create a negative load factor. The value of α' is taken to be 8° in the current work which results in the wing providing a significant portion of the vehicle in the climbing stage of the manoeuvre whilst maintaining an adequate stall margin. The fuselage angle of attack variation is described by a fifth order polynomial, similar to that of Equation 13, therefore the angle of attack time derivative, $\dot{\alpha}$, is easily obtained through differentiation.

ADS-33 Accel-Decel Maneuver

The Accel-Decel manoeuvre starts with the aircraft in the hover. It then accelerates to a flight velocity of 50 kt before aggressively decelerating back to a stabilized hover. The objective of this manoeuvre is to examine the pitch and heave axis handling qualities [28]. As the initial heading of the aircraft is to be maintained throughout the manoeuvre, the track angle, χ, and heading rate, $\dot{\psi}$ is set to zero. The five boundary conditions of this manoeuvre are given in Table 2 with the assumption that the maximum flight velocity of 50 kt is reached at the half-way point. A fourth-order polynomial describes the flight velocity

$$V(t) = b_0 t^4 + b_1 t^3 + b_2 t^2 + b_3 t + b_4 \tag{15}$$

where b_0, b_1, b_2, b_3 and b_4 are coefficients which are determined by applying the boundary conditions. For this particular manoeuvre, $\dot{x} = V(t)$ whereas $\dot{y} = \dot{z} = 0$. The rate of change of the flight velocity is readily available through the differentiation of Equation (15), therefore allowing the calculation of the accelerations which are contained in the output vector, $\mathbf{y}_{des}$. The manoeuvre is defined by setting the distance to be travelled, S, obtained by integration of Equation (15) rather than specifying t_{end}.

The approach taken to calculate the control activity of the HCH configuration throughout the Accel-Decel maneuver is to schedule the propeller pitch control during the manoeuvre so that the output vector consists of four elements. These are the three accelerations in the Earth axes set and the heading rate. As the propeller pitch is known throughout the manoeuvre, there are four unknown controls to calculate at each time point. The pitch schedule is developed to maximize the propeller thrust in the acceleration portion of the manoeuvre and is lowered in the deceleration segment. This manner of scheduling the propeller

Table 2. Accel-Decel Boundary Conditions.

Variable	$t = 0s$	$t = t_{end}/2$	$t = t_{end}$
V	0	50 kt	0
$\dot{V}$	0	0	0

pitch is likely to be similar to the control strategy that the pilot would adopt to fully exploit the addition of propellers to the aircraft design. Of course, the pilot actively using five controls would undoubtedly increase the pilot workload throughout the manoeuvre. A solution to this issue could be a control system and interface, whereby the pilot has four available controls with a control system automatically altering the propeller pitch to increase propeller thrust in the acceleration segment of the manoeuvre. Such an investigation is not considered in the current work.

Manoeuvrability of the Configurations

The inverse simulation technique has been used to assess both the manoeuvrability and agility of helicopters [17, 30]. In this current work, a similar approach to Whalley's is adopted [17], in order to assess the maximum manoeuvring capability of two helicopter configurations. However, there are some differences. Firstly, the integration method is used within this work unlike the differentiation technique used by Whalley [17]. The integration method has proven to be a robust and flexible approach which separates the mathematical model and the inverse simulation algorithm. This method also permits the inclusion of high fidelity modelling techniques, such as individual rotor blade modelling, which are not included within this study of compound helicopters but could be in future work.

Another important difference between Whalley's work and the current approach is the definition of the limiting factor which determines the aircraft's ability to complete a manoeuvre. There are various

limits which define the manoeuvrability of a rotorcraft, which include aerodynamic, power and control travel limits [31]. In Whalley's work [17] it is assumed that the maximum or minimum control angles are the limiting factor for the helicopter configuration to perform a particular manoeuvre. Indeed this can be selected to be manoeuvrability limit in this work, however due to the assumption of linear aerodynamics within the current rotor model and therefore not modelling blade stalling, the extreme limit of the main rotor collective can be reached producing an unrealistic amount of rotor thrust. The first solution to this is to assume that the aerodynamic limitations of the main rotor determine the maximum manoeuvring capability of the vehicle. Hence, it is assumed that the limiting factor of certain manoeuvres occurs when the local angle of attack of the rotor blades, at a radial position $\bar{r} = 0.8$ is equal to 12° at any time point or azimuth position. The selection of the local maximum angle of attack of 12° is chosen as it is approximately the highest local blade angle of angle where the assumption of linear aerodynamics is valid. Whereas a radial position of $\bar{r} = 0.8$ represents the outer portion of the blades where airloads generally tend to be at their highest. These selected values of maximum local blade angle of attack and radial position have been altered in simulation runs to investigate their influence in the final manoeuvrability results. The analysis showed that as long as the radial position represented the outer portion of the rotor blades (i.e. $\bar{r} > 0.7$) then there was no significant difference in the final results. A similar result was found in the maximum local angle of attack selection, if the selected value was in the interval of 10-14°. An alternative approach is to assume that the power available restricts the vehicle's ability to complete a manoeuvre. This approach seems appropriate for certain manoeuvres which involve a compound helicopter. For example, in certain manoeuvres the wing offloads the main rotor and therefore it is unlikely that the aerodynamic restrictions of the main rotor would determine the vehicle's manoeuvrability. For these reasons, the manoeuvrability method allows the user to select their assumed limit which can based on control travel limits, main rotor aerodynamic restrictions or the power available.

Figure 3 presents an overview of the Manoeuvrability Assessment Method (MAM). This iterative method uses inverse simulation to determine the maximum manoeuvring capability of the two aircraft configurations. The method begins at the first iterative counter and subsequently defines the manoeuvre. Thereafter, the integration method calculates the control angles required to force the particular aircraft configuration along the desired flight path. With the controls and states calculated throughout the ma-

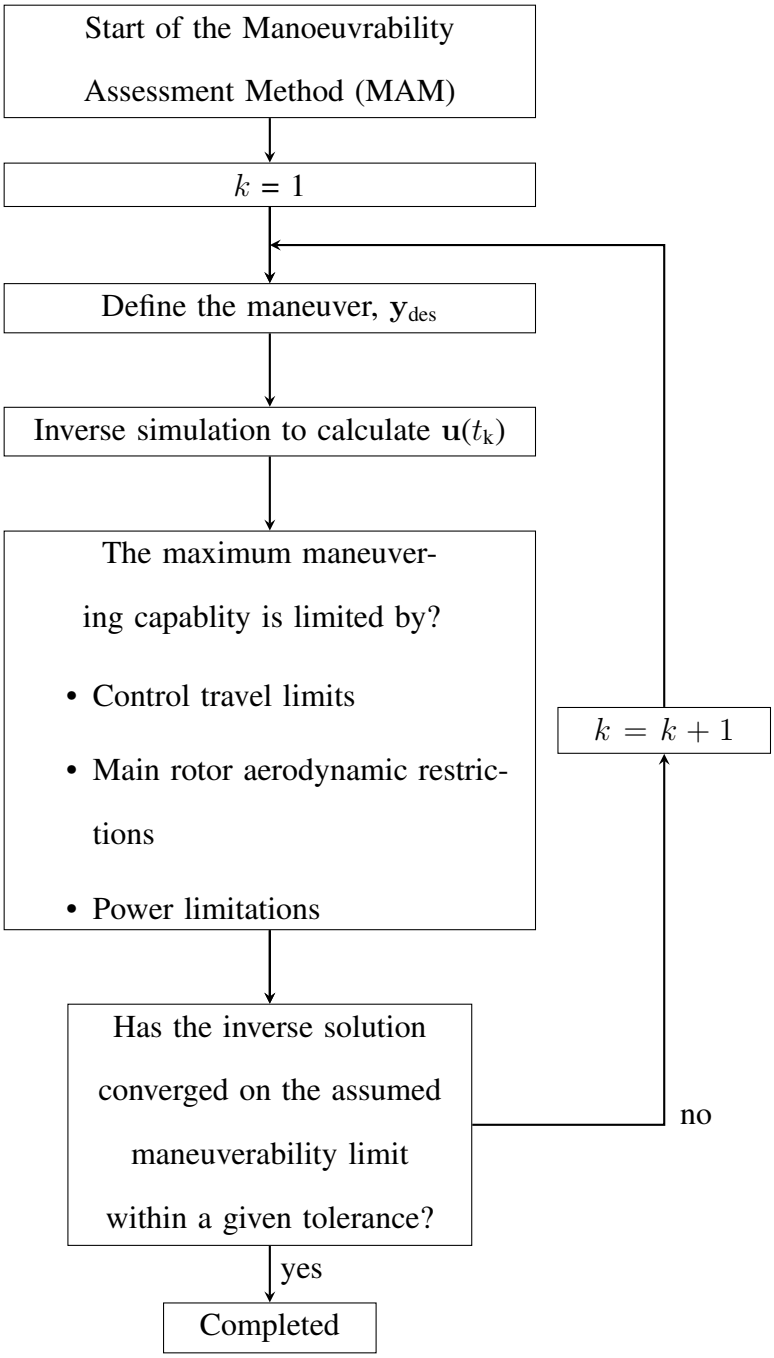

Fig. 3 Flowchart Describing the Manoeuvrability Assessment Method.

noeuvre, the assumed limiting factor determining the vehicle's manoeuvrability can be calculated. If the limit is selected to be the aerodynamic restrictions of the main rotor then the local angle of attack at every time point, around the azimuth and at a radial position of $\bar{r} = 0.8$ is calculated. If $\alpha_{max} < 12$ at $\bar{r} = 0.8$, at any time point throughout the manoeuvre then the aggressiveness of manoeuvre is redefined until this con-

dition is satisfied. Conversely, if the power available is the limiting factor then the total power throughout the manoeuvre is calculated and then the manoeuvre is redefined until MAM converges towards a solution. In terms of the Pullup-Pushover manoeuvre, the variable n_{max} in the manoeuvre definition, is allowed to alter the aggressiveness of the manoeuvre and therefore converge towards the manoeuvrability limit. Whereas with the Accel-Decel manoeuvre, the distance travelled by the vehicles, S, is varied to converge towards a solution. The manoeuvrability limit is generally reached within 5 iterations.

Results

Maneuverability Results

With the methodology developed, MAM can now be used to predict the manoeuvrability of the two aircraft configurations. For the Pull-Pushover manoeuvre, the assumed limiting factor which influences the HCH configuration's manoeuvrability is the power required. In the climbing portion of the manoeuvre, the wing offloads the main rotor, therefore it is unlikely that the main rotor's aerodynamic restrictions would be the limiting factor for this particular manoeuvre. Conversely, the aerodynamic restrictions of the main rotor is assumed to be the BL configuration's limiting factor.

Concerning the BL configuration, Figure 4 presents the maximum calculated local blade angle of attack around the azimuth at each time point at the radial position, $\bar{r}$ = 0.8. Also shown is the total power of the HCH configuration which is assumed to be limiting factor influencing the vehicle's manoeuvrability in this manoeuvre. As expected, the predicted limiting state of the BL configuration's main rotor occurs as the vehicle sustains its greatest normal load factor at ≈3s. In a similar manner the power of the HCH configuration reaches 1400kW at this time which equals the power available, therefore predicting the vehicle's manoeuvrability. The load distributions achieved by each vehicle are shown in Figure 5(a). The maximum load factors achieved by the HCH and BL configurations are 2.16 and 1.88, respectively. As a consequence the HCH configuration climbs to a greater height than the BL configuration, with the height profiles of the two configurations shown in Figure 5(b). The HCH configuration reaches a height of 180m after 8s whereas the BL configuration's maximum height is 99m is attained at 7.1s.

Figure 6 shows the predicted control displacements throughout the maximum Pullup-Pushover ma-

noeuvres. In the first second of the manoeuvre, a large main rotor collective control input is required by the BL configuration to transition to a positive load factor. However, there is little movement of the HCH configuration's collective within the early stages of the manoeuvre. In contrast, there is a large initial longitudinal stick input to pitch the HCH configuration's nose up thereby increasing the lifting force provided by the wing. In addition, there is a rapid rise in the mean propeller pitch setting, $\bar{\theta}_{prop}$, within the first second of the initial control input to increase the propulsive force of the two propellers. Therefore, initially the required rotor thrust of the HCH configuration is less than that of the BL configuration, consequently lowering the main rotor collective input required. After one second the trend of the longitudinal stick displacements are similar for the two aircraft configurations. As the vehicles transition to their minimum load factors, both assumed to be 0, the main rotor collective levers drop to lower the level of rotor thrust. The longitudinal cyclic of the BL configuration reaches its minimum value at 4.5s as it pitches down the

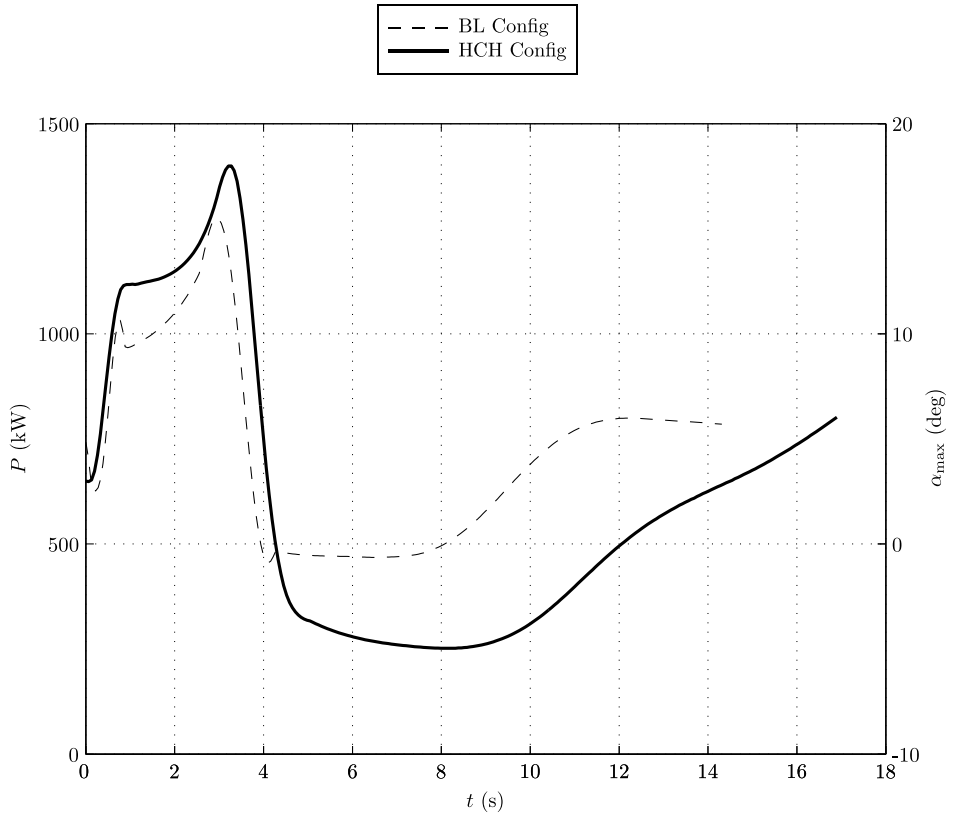

Fig. 4 Maximum Local Blade Angle of Attack Variation and Power during the Maximum Pullup-Pushover Manoeuvre.

aircraft to achieve a zero normal load factor. The propeller pitch control input is fairly constant between 1-3s as the HCH configuration sustains its positive load factor. However, as the aircraft transitions to a pushover the control input reduces significantly from 50° to a value of 31°. The control remains within this region until it is increased in the latter stages of the manoeuvre to recover the vehicle's original airspeed. Note that the additional constraint featured in the HCH configuration's output vector, chosen to be the fuselage angle of attack, results in a more gradual change of pitch attitude when compared to the BL configuration.

For the Accel-Decel manoeuvre, the aerodynamic restrictions of the two main rotors are assumed to be limiting factor influencing the manoeuvrability of the two aircraft configurations. Figure 7 shows the maximum calculated local blade angle of attack around the azimuth at each time point at the radial position, $\bar{r}$ = 0.8. The two configurations reach their limiting states, i.e. $\alpha_{max} = 12$, at approximately 1s, highlighting that MAM has successfully found a solution. This point corresponds to an aggressive part of the manoeuvre whereby there are large collective and longitudinal control inputs for both configurations to accelerate the vehicles from the hover. The predicted result is that the two aircraft configurations complete the manoeuvre in comparable time-scales, with the BL and HCH configurations completing the

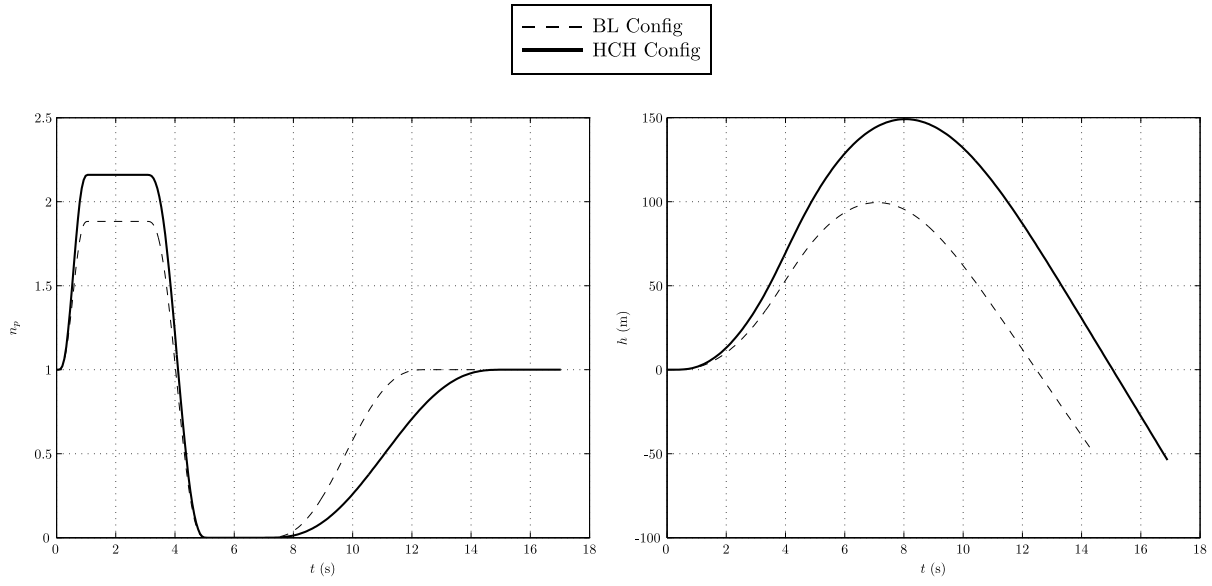

(a) Load Factor Distribution (b) Height Profile

Fig. 5 Flight path during the Pullup-Pushover Manoeuvres.

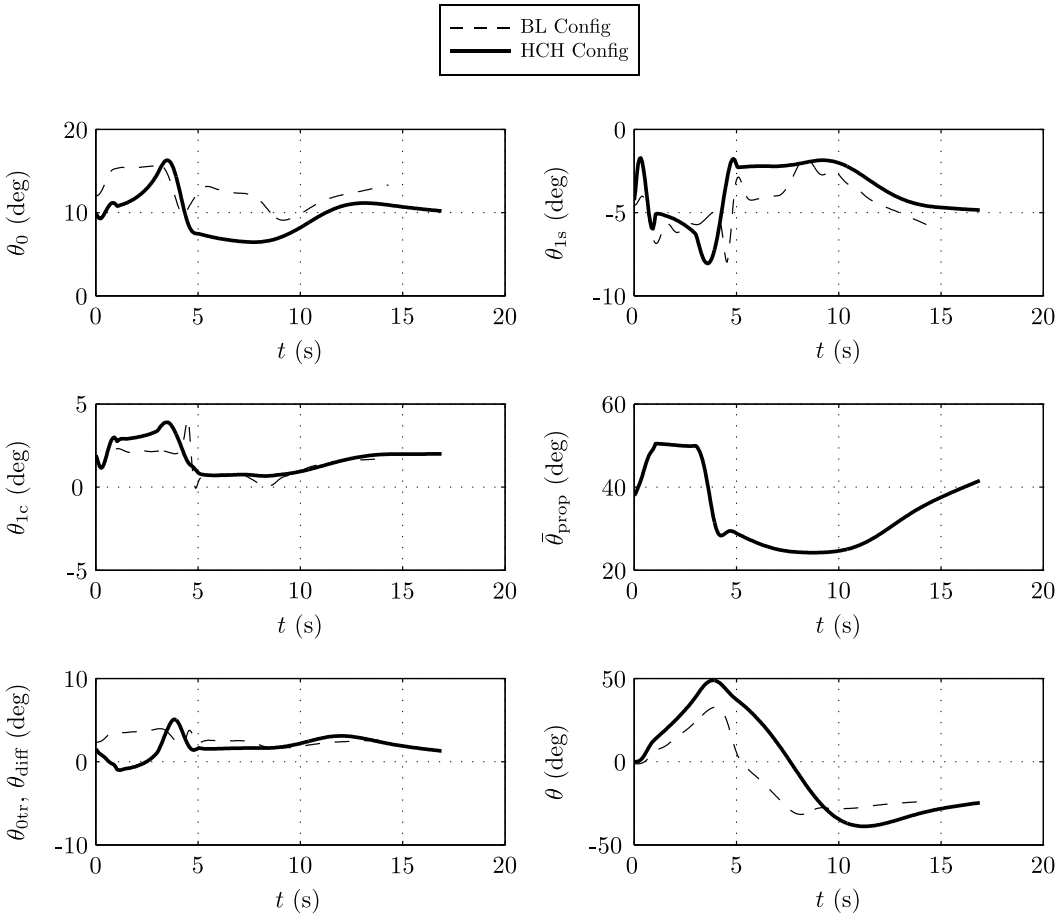

Fig. 6 Maximum Manoeuvrability Control time histories of the HCH and BL configurations during the Pullup-Pushover maneuver.

manoeuvre in 8.7s and 8.85s, respectively. Figure 8 shows the longitudinal distance travelled by the two vehicles, with the BL configuration completing the manoeuvre over a distance of 120.8m, whereas the HCH configuration covers a total distance of 121.9m. This result suggests that there is little difference in the predicted maximum manoeuvring capability whilst performing this manoeuvre. One possible reason for this is that the wing provides an aerodynamic download at these low flight speeds, requiring greater collective inputs in the early stage (between 0-1s) of the manoeuvre. Another explanation is the low levels of propeller thrusts required in the stabilized hover. As the manoeuvre commences the mean propeller pitch setting, $\bar{\theta}_{prop}$, has to be increased significantly, which takes a few seconds, to provide a sizeable propulsive force. By the time the propellers produce significant axial thrust, $\approx$ 3s, there has already been large cyclic control pitch inputs which lead to the main rotor reaching its limiting state. However the ad-

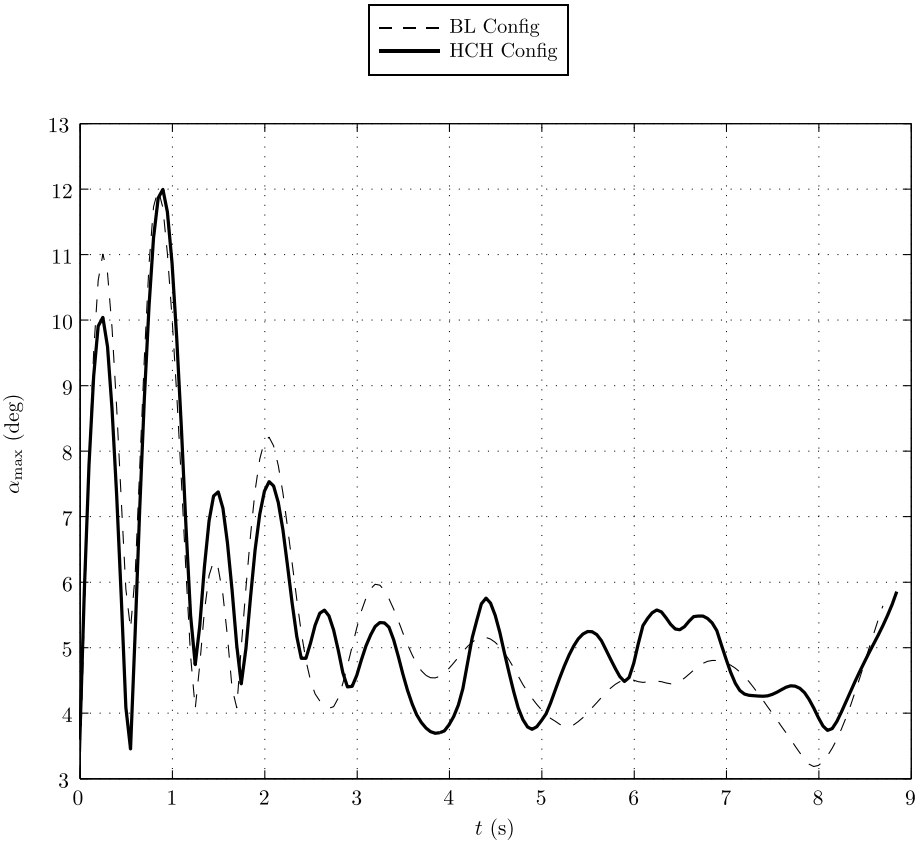

Fig. 7 Maximum Local Blade Angle of Attack Variation during the Maximum Accel-Decel Maneuver.

dition of thrust compounding, featured in the HCH configuration, attenuates the pitch attitude excursions in the acceleration stage of the manoeuvre. This is clearly a beneficial aspect of the helicopter design.

Figure 9 presents the control time histories throughout the maximum Accel-Decel manoeuvres. As noted previously, the mean propeller pitch, $\bar{\theta}_{prop}$, is scheduled throughout this manoeuvre so that a unique solution can be determined at each time point but more importantly so that the HCH configuration exploits the benefit of thrust compounding. This manner of scheduling the propeller pitch allows the propulsive force of the two propellers to be controlled throughout the manoeuvre. The propeller pitch schedule, as seen in Figure 9, results in the two propellers providing a significant propulsive force in the early stages of the manoeuvre to provide axial acceleration, with the starboard and port propellers reaching maximum thrusts of 11.6kN and 6.4kN, respectively at the time of maximum acceleration. Note this manner of propeller pitch scheduling assumes that the no significant reverse thrust is used in the deceleration stage of the manoeuvre. At the starting position of the manoeuvre the main collective of the HCH con-

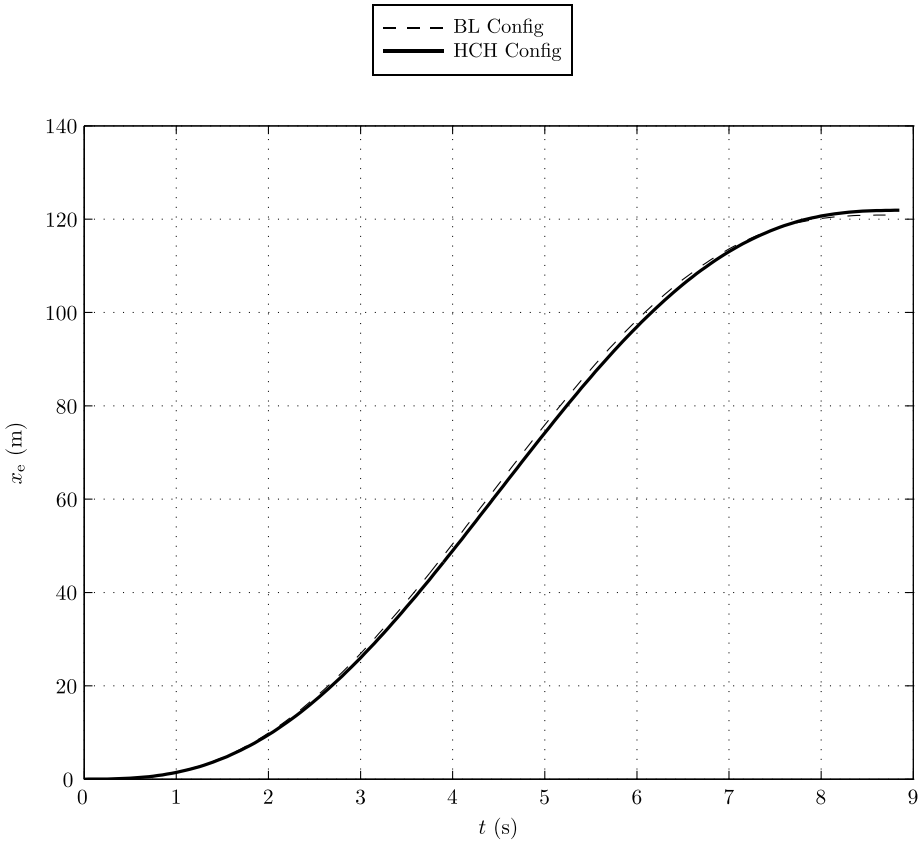

Fig. 8 Flight path of the Maximum Accel-Decel Maneuvers.

figuration is greater than that of the BL configuration. This is due to wing of the HCH configuration providing an aerodynamic download which requires collective to offset the download force. As the manoeuvre commences, the main rotor collective of the two configurations increase with the collective of the BL configuration reaching its highest value at 4s. The HCH configuration's highest collective setting is reached at a much shorter time of 2s. When the main rotor collective of HCH configuration reaches its peak, the two propellers are producing a significant portion of the propulsive thrust to accelerate the aircraft. For a conventional helicopter the main rotor is responsible for both the propulsive and lifting capability of the vehicle [31]. One undesired quality of the helicopter is that in order to accelerate or decelerate a large pitch excursion is required. As a consequence, after 2s the main rotor disc of the HCH configuration does not have to tilt as much as the BL configuration in order to provide the propulsive force to the accelerate the vehicle. The net effect is that the pitch attitude is reduced, between 1-4s, when the pitch attitude of the two configurations are compared, highlighting one of the benefits of thrust com-

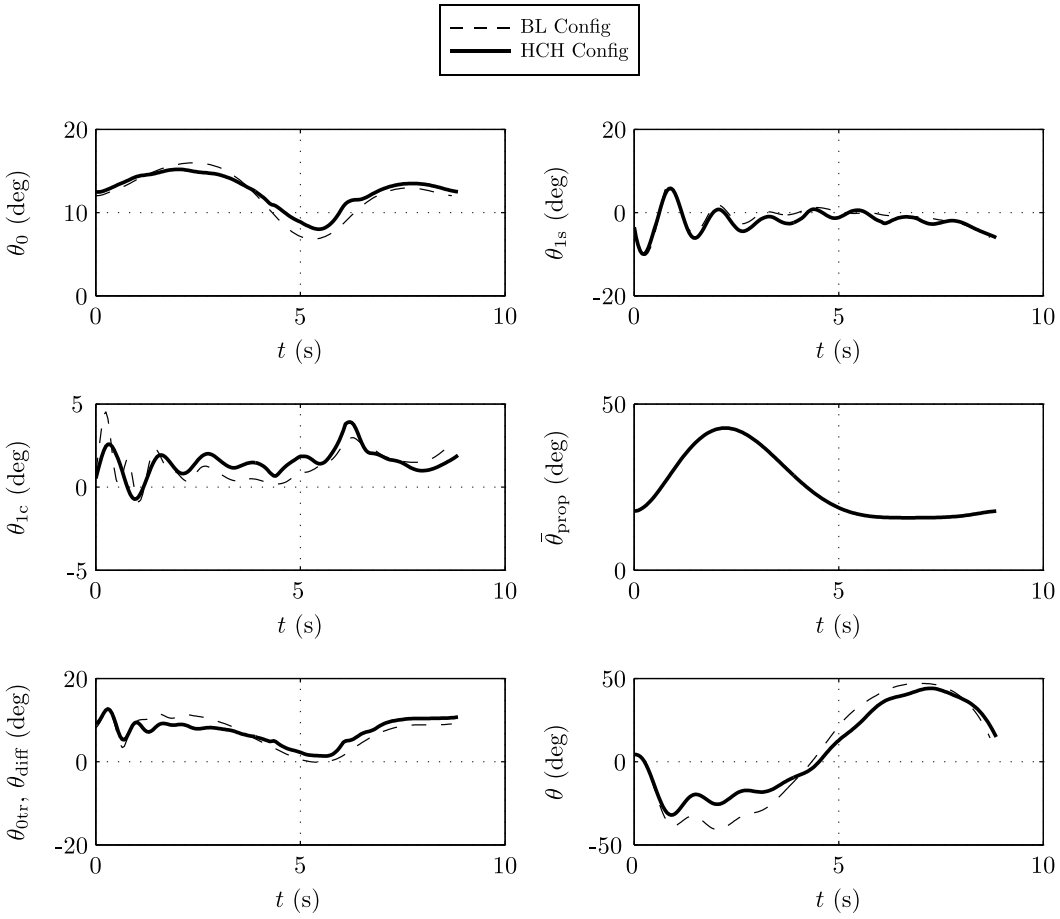

Fig. 9 Maximum Manoeuvrability Control time histories of the HCH and BL configurations during the Accel-Decel manoeuvre.

pounding. The main rotor cyclic inputs are very similar throughout the manoeuvre. Both configurations exhibit large oscillatory longitudinal cyclic control inputs at the beginning of the manoeuvre. In terms of the anti-torque controls, θ_{0tr} and θ_{diff}, their control time histories are similar to the collective settings in order for the aircraft configurations to retain a constant heading.

Conclusions

The manoeuvrability of a hybrid compound helicopter and a conventional helicopter have been examined. The following is a list of the main conclusions drawn from this work:

- A preliminary manoeuvrability assessment of a hybrid compound helicopter has been conducted. When comparing the main rotor collective displacements of the configurations in the initial stages

of the Pullup-Pushover manoeuvre, the HCH configuration requires less collective input than the BL configuration. This is due to the wing offloading the main rotor as the aircraft climbs to achieve a positive load factor and the two propellers providing significant propulsive thrust. The combination of these two types of compounding reduces the amount of rotor thrust required therefore lowering the amount of main rotor collective required. In addition, the introduction of the additional constraint, $\dot{\alpha}$, to calculate the control displacements of the HCH configuration results in a gradual change in pitch attitude as the aircraft transitions from the maximum load factor to the minimum. In terms of manoeuvrability, the HCH configuration is able to achieve a greater load factor than the BL configuration. This is primarily due to the combination of thrust and wing compounding offloading the main rotor's propulsive and lifting duties throughout the manoeuvre.

- For the Accel-Decel manoeuvre, the cyclic control activity of the two configurations is similar throughout the manoeuvre. The addition of thrust compounding lowers the required pitch attitude of the vehicle in the forward acceleration stage of the manoeuvre as expected. As the main rotor does not have to provide the propulsive force the tilt of the rotor disc is smaller than that of the BL configuration, attenuating the pitch attitude. Regarding the manoeuvrability of the two configurations, there is little difference in the predicted maximum manoeuvrability of the two vehicles performing this manoeuvre. This is due to the large longitudinal oscillatory stick inputs of the two configurations in the early stages of the manoeuvre. These control inputs lead to the estimated limiting state of the two main rotors.

Acknowledgements

The authors would like to acknowledge the Scottish Funding Council (SFC) for providing the funding, under the GRPE Scholarship, to conduct this research.

References

[1]Orchard, M. and Newman, S., "The compound helicopter - why have we not succeeded before?" *The Aeronautical Journal*, Vol. 103, (1028), 1999, pp. 489–495.

[2]Thomson, D. and Bradley, R., "Inverse simulation as a tool for flight dynamics research - Principles and applications," *Progress in Aerospace Sciences*, Vol. 42, (3), May 2006, pp. 174–210.
doi: 10.1016/j.paerosci.2006.07.002

[3]Thomson, D. and Bradley, R., "An analytical method of quantifying helicopter agility," Proceedings of the 12th European Rotorcraft Forum, 1986.

[4]Thomson, D. and Bradley, R., "An investigation of pilot strategy in helicopter nap-of-the-earth manoeuvres by comparison of flight data and inverse simulation," Royal Aeronautcal Society: helicopter handling qualities and control, 1988.

[5]Thomson, D. and Bradley, R., "The use of inverse simulation for conceptual design," 16th European Rotorcraft Forum, 1990.

[6]Thomson, D. and Bradley, R., "The use of inverse simulation for preliminary assessment of helicopter handling qualities," *The Aeronautical Journal*, Vol. 101, (1007), 1997, pp. 287 – 294.

[7]Cameron, N., Thomson, D., and Murray-Smith, D., "Pilot modelling and inverse simulation for initial handling qualities assessment," *The Aeronautical Journal*, Vol. 107, (1074), 2003, pp. 511– 520.

[8]Hess, R., Gao, C., and Wang, S., "Generalized technique for inverse simulation applied to aircraft maneuvers," *Journal of Guidance, Control and Dynamics*, Vol. 14, (5), 1991, pp. 920–926.
doi: 10.2514/3.20732

[9]Hess, R. and Gao, C., "A Generalized Algorithm for Inverse Simulation Applied to Helicopter Maneuvering Flight," *Journal of the American Helicopter Society*, Vol. 38, (4), 1993, pp. 3 – 15.
doi: 10.4050/JAHS.38.3

[10]Avanzini, G., de Matteis, G., and de Socio, L., "Two-Timescale-Integration Method for Inverse Simulation," *Journal of Guidance, Control and Dynamics*, Vol. 22, (3), 1999, pp. 395–401.
doi: 10.2514/2.4410

[11]Avanzini, G. and de Matteis, G., "Two-timescale inverse simulation of a helicopter model," *Journal of Guidance, Control and Dynamics*, Vol. 24, (2), 2001, pp. 330–339.
doi: 10.2514/2.4716

[12]Celi, R., "Optimization-Based Inverse Simulation of a Helicopter Slalom Maneuver," *Journal of*

Guidance, Control and Dynamics, Vol. 23, (2), 2000, pp. 289–297.
doi: 10.2514/2.4521

[13]de Matteis, G., de Socio, L., and Leonessa, A., "Solution of Aircraft Inverse Problems by Local Optimization," *Journal of Guidance, Control and Dynamics*, Vol. 18, (3), 1995, pp. 567–571.
doi: 10.2514/3.21424

[14]Olson, J. and Scott, M., "Helicopter Design Optimization for Maneuverability and Agility," American Helicopter Society 45th Annual Forum, 1989.

[15]Johnson, K., *Prediction of Operational Envelope Maneuverability Effects of Rotorcraft Design*, Ph.d, Georgia Institute of Technology, 2013.

[16]Levine, L., Warburton, F., and Curtiss Jr, H., "Assessment of Rotorcraft Agility and Maneuverability with Pilot-in-the-loop Similation," American Helicopter Society 41st Annual Forum, 1985.

[17]Whalley, M., "Development and Evaluation of an Inverse Solution Technique for Studying Helicopter Maneuverability and Agility," USAAVSCOM TR 90-A-008, 1991.

[18]Padfield, G., *Helicopter Flight Dynamics: the Theory and Application of Flying Qualities and Simulation Modelling*, Blackwell Publishing, second edition, 2007.

[19]Ferguson, K. and Thomson, D., "Flight dynamics investigation of compound helicopter configurations," *Journal of Aircraft*, Vol. AIAA Early Online Edition, 2014.
doi: 10.2514/1.C032657

[20]Thomson, D., "Development of a Generic Helicopter Mathematical Model for Application to Inverse Simulation," Internal Report No. 9216, Department of Aerospace Engineering, University of Glasgow, UK, 1992.

[21]Kim, F., Celi, R., and Tischler, M., "Forward flight trim and frequency response validation of a helicopter simulation model," *Journal of Aircraft*, Vol. 30, (6), 1993, pp. 854–863.
doi: 10.2514/3.46427

[22]Rutherford, S., *Simulation Techniques for the Study of the Manoeuvring of Advanced Rotorcraft Configurations*, Phd thesis, University of Glasgow, 1997.

[23]Mansur, M., "Development and Validation of a Blade Element Mathematical Model for the AH-64A Apache Helicopter," NASA-TM-108863, 1995.

[24]Houston, S., "Validation of a non-linear individual blade rotorcraft flight dynamics model using a perturbation method," *The Aeronautical Journal*, Vol. 98, (977), 1994, pp. 260–266.

[25]Bradley, R., Padfield, G., Murray-Smith, D., and Thomson, D., "Validation of helicopter mathematical models," *Transactions of the Institute of Measurement and Control*, Vol. 12, (186), 1990.
doi: 10.1177/014233129001200405

[26]Rutherford, S., *Simulation Techniques for the Study of Advanced Rotorcraft*, Ph.d thesis, University of Glasgow, 1997.

[27]Thomson, D. and Bradley, R., "Mathematical Definition of Helicopter Maneuvers," *Journal of the American Helicopter Society*, Vol. 4, (1), 1997, pp. 307 – 309.
doi: 10.4050/JAHS.42.307

[28]Anon., "Handling qualities requirements for military rotorcraft," Aeronautical design standard ADS-33E-PRF, United States army aviation and troop command, 2000.

[29]Celi, R., "Analytical Simulation of ADS-33 Mission Task Elements," American Helicopter Society 63rd Annual Forum, 2007.

[30]Thomson, D., *Evaluation of helicopter agility through inverse solution of the equations of motion*, Ph.d, University of Glasgow, 1987.

[31]Leishman, J., *Principals of Helicopter Aerodynamics*, Cambridge University Press, second edition, 2006.

List of Figures

List of Tables